International Journal Of
Industrial Electronics Control and Optimization
Print ISSN: 3517-2645
Online ISSN: 3568-2645
Homepage: https://ieco.usb.ac.ir/

A New Protection Strategy for Microgrid based on Integration of Active Power Index and Fault Current Differential Energy

Reza Karimi[1], Abbas Ketabi[2], Seyyed Moammad Nobakhti[3]

Department of Electrical and Computer Engineering, University of Kashan, 6 km Ghotbravandi Blvd, Postal Code: 8731753153, Kashan, Iran [1,2]
Department of Electrical Engineering, National University of Skills (NUS), Tehran, Iran[3]
Corresponding author's email: aketabi@kashanu.ac.ir

Article Info

Article type:
Research Article

Article history:
Received: 27-July-2024
Received in revised form: 15-September-2024
Accepted: 03-October-2024
Published online: 23-Sep-2025

Keywords:
Active power flowing,
Distributed generation,
Energy difference signal,
Fault current direction,
Microgrid protection.

ABSTRACT

The integration of distributed generation (DG) sources into distribution systems has experienced significant growth due to their numerous advantages. However, DG integration has also introduced substantial challenges to distribution system protection, such as variations in fault current levels and bidirectional fault current flow. Under these conditions, directional overcurrent relays may not operate as intended. This paper proposes a directional comparison protection scheme for safeguarding lines and zones in active distribution systems, based on the calculation of incremental active power transient energy. Additionally, a differential protection scheme, based on the Teager–Kaiser Energy Operator (TKEO), is incorporated to enhance the performance of the directional identification algorithm. The proposed scheme is capable of detecting symmetric and unsymmetric faults on microgrid lines at both low and medium voltage levels and is adaptable to changes in microgrid configurations and load-switching transients. The proposed methods offer the advantages of simplicity in calculation and high accuracy. An AC active distribution system incorporating inverter-based DG sources is modeled in PSCAD-EMTDC software to simulate various fault types, and the simulation results are subsequently transferred to MATLAB for the implementation of the proposed algorithms.

I. Introduction

Electricity has been a fundamental requirement for human society since the early stages of civilization. The rapid growth in electricity consumption has significantly impacted energy resources, particularly fossil fuels, leading to a decline in these reserves. In addition, the increase in fossil fuel consumption and the associated undesirable environmental effects have created a basis for the development and use of renewable energy. The deployment of distributed generation resources in distribution systems has increased markedly in recent years. Distributed generation resources are those located at or near the point of electricity consumption and inject their generated electricity directly into the distribution grid. Distributed generation (DG) resources offer several advantages over centralized generation resources. The reduction of distribution network losses is one of the most important advantages of distributed generation (DG) resources, as they are typically located near the point of consumption, which reduces the distance that electricity must travel through the network. Distributed generation (DG) resources can significantly improve the reliability of the power grid by providing a local source of backup power in the event of a power outage from centralized generation sources. DG resources can also enhance the stability of a power grid by supplying local, flexible, and responsive power during periods of increased grid load. The use of renewable energy sources for electricity generation can lead to a significant reduction in air pollution and environmental impacts. The rapid growth of distributed generation resources in distribution systems has created conditions for the development and operation of microgrids. The emergence of microgrids, which are small-scale power systems, has revolutionized the landscape of electricity supply. These innovative systems harness local generation resources such as solar, wind, and small-scale generators, offering a sustainable and flexible solution for regions lacking access to the main grid or facing grid constraints.

Microgrids, while capable of connecting to the main grid, also possess the ability to operate in island mode. This capability eliminates over-reliance on the central grid, significantly enhancing system stability and security. Microgrids can be broadly categorized into two types based on their connection to the main grid:

1. Grid-Connected Microgrids: Grid-connected microgrids establish a connection with the main grid, enabling them to exchange power with the broader electricity network. This bidirectional power flow allows these microgrids to: Supplement Electricity Supply: During periods of peak demand, grid-connected microgrids can draw power from the main grid to meet local electricity needs. Inject Excess Generation: Conversely, when microgrid generation exceeds local demand, surplus electricity can be injected into the main grid, contributing to overall grid stability and resource optimization. Grid-connected microgrids are particularly well-suited for electrifying remote areas and regions with weak or unreliable grid infrastructure.

They offer several advantages, including:

Enhanced System Stability and Security: The ability to draw power from the main grid during disturbances ensures uninterrupted power supply to critical loads. Reduced Reliance on Central Grid: By generating and consuming electricity locally, grid-connected microgrids lessen dependence on the main grid, increasing energy autonomy. Improved Power Quality: Active regulation of voltage and frequency within the microgrid enhances power quality for consumers. Increased Flexibility and Efficiency: Real-time energy management and optimization enable grid-connected microgrids to respond effectively to demand fluctuations and optimize resource utilization.

2. Island Microgrids: Island microgrids operate autonomously, disconnected from the main grid. They rely solely on local generation resources to meet their electricity needs. This self-sufficiency provides several benefits, particularly in remote or grid-constrained areas: Uninterrupted Power Supply: Island microgrids are immune to disruptions in the main grid, ensuring a continuous and reliable power supply for critical infrastructure and communities. Energy Independence: By generating electricity locally, island microgrids eliminate reliance on imported fossil fuels, promoting energy independence and sustainability. Resilience in Remote Locations: Island microgrids provide a stable power source for remote areas that are difficult or expensive to connect to the main grid.

Despite their advantages, island microgrids also present certain challenges: Higher Initial Investment: The upfront costs of establishing an island microgrid, including local generation and storage infrastructure, can be higher compared to grid-connected systems. Need for Advanced Control Systems: Island microgrids require sophisticated control and management systems to ensure real-time balancing of supply and demand and to maintain grid stability. Limited Scalability: The capacity of island microgrids is typically constrained by local generation resources, limiting their ability to serve large-scale loads. In addition to the categorization of microgrids based on their grid connection type and location, another classification scheme exists based on the type of power transfer employed within the microgrid. This classification encompasses three primary microgrid types:

1. AC Microgrids: In AC microgrids, all system components, including generation sources, loads, and transmission lines, utilize alternating current (AC) for power transmission. AC, as the prevalent standard in the electricity industry, offers advantages such as simplicity of structure, ease of connection to existing power grids, and high efficiency in power transmission over long distances.

2. DC Microgrids: DC microgrids employ direct current (DC) for power transmission throughout the system's components. DC presents benefits such as lower losses over short distances, compatibility with renewable energy generation sources like solar panels and batteries, and enhanced controllability and manageability.

3. Hybrid Microgrids: Hybrid microgrids represent a combination of AC and DC microgrids. In this type of microgrid, both AC and DC are utilized for power transmission in different parts of the system. This approach simultaneously harnesses the advantages of both AC and DC systems, leading to increased flexibility and efficiency within the microgrid.

Microgrid Selection: Selecting the appropriate microgrid type depends on various factors, including the nature of generation sources, load types, transmission line lengths, and the control and protection requirements of the system. In certain scenarios, employing a combination of AC and DC microgrids, forming a hybrid microgrid, may constitute a more optimal solution. The impact of these resources on the performance of protective systems has also increased with the growing penetration of distributed generation resources (DGs) in power distribution networks. Among the most significant impacts of DGs on the protection of distribution systems are the following: Voltage variations: DGs are typically small-scale and installed at various points in the distribution network. Therefore, they may cause variations in the network voltage levels, which can lead to disruptions in the network and equipment damage. Influence of distributed generation on network losses: Distributed generation can cause either a reduction or an increase in network losses, depending on the capacity, location, and type of distributed generation. Changes in network losses can lead to improper operation of protective equipment. The structure of distributed generation (DG), the reduced level of fault current in islanded mode, the change in fault current level with the transition of microgrid mode from connected to disconnected, and the low inertia of microgrids are all factors

that affect the protection of active distribution systems and the performance of directional overcurrent relays.[17]. The structure of DG can influence the magnitude of the fault current. DG connected to the distribution system through a point of common coupling (PCC) can increase the fault current. However, DG isolated from the distribution system or connected to the distribution system through a microgrid can reduce fault current [18-20]. In islanded mode, the DG can lower the fault current by providing a local source of power. This can impact the operation of the overcurrent relays, which are designed to function based on the magnitude of the fault current. Microgrids can operate in either connected or islanded mode. In connected mode, the microgrid is linked to the distribution system. In islanded mode, the microgrid is isolated from the distribution system [13, 19]. The change in the microgrid mode from connected to islanded can alter the magnitude of fault current. This is because the distributed generation (DG) connected to the microgrid can provide a local source of power in the islanded mode. Microgrids with low inertia are more vulnerable to faults, as they can experience larger transient overvoltage and overcurrent during a fault [16]. Despite the operational challenges associated with the use of distributed energy resources (DERs) in distribution systems, their unique benefits are clear. These benefits include reduced energy loss, improved network stability, and increased power supply reliability. Consequently, researchers have been investigating the effects of DERs on distribution systems and have provided various solutions for the optimal utilization of these resources. The authors in [17] propose a multi-agent system-based protection scheme for protecting distribution systems that contain distributed generation resources. The proposed scheme can achieve satisfactory performance for protection under low-impedance fault conditions. In [21], a wave-polarity-based protective technique for fault detection is proposed. This technique can accurately and quickly detect faults by comparing the polarities of the traveling waves at two points in the network. A protection scheme for locating faults in radial distribution systems is proposed in [22]; however, it does not function properly when distributed generation resources are utilized. Moreover, the proposed scheme does not perform well in radial distribution systems with increased fault impedance. In [23], an automatic coordination mechanism based on the exchange of information was used to achieve coordination between the overcurrent relays. This mechanism automatically establishes coordination between relays using current and voltage information at the relay connection point. The main challenge of this mechanism is the need for a telecommunications infrastructure to exchange information between relays. In [24], an adaptive protection scheme based on non-standard characteristic curves was proposed. This scheme can provide satisfactory protection performance under various network conditions by leveraging the flexibility of non-standard characteristic curves. However, this scheme has a major drawback in that it does not consider islanding performance. In [19], the authors proposed a novel protection scheme based on the optimization of relay parameters by considering multiple characteristic curves for directional overcurrent relays. This scheme can provide satisfactory protection under various network conditions. In [25], a novel method was proposed for identifying single-phase faults in active power distribution systems using zero- and negative-sequence current. This method can identify single-phase faults under various network conditions by utilizing the features of zero- and negative-sequence currents. Considering the impact of solid-state transformers on the coordination of overcurrent relays, the authors in [5] introduced a novel protection scheme. However, it fails to operate under conditions with inverter-based distributed generation resources and high-impedance faults. In [26], the authors propose a novel adaptive optimization method for directional overcurrent relay coordination to achieve optimal protection coordination in microgrids with diverse topologies. This innovative approach utilizes advanced optimization algorithms to optimally adjust relay parameters under various network conditions, ensuring robust protection coordination against a wide range of faults. The method first employs powerful feature extraction algorithms to extract the characteristics of zero-sequence and negative-sequence currents. Subsequently, these extracted features are fed into an advanced prediction model to accurately estimate the fault probability at different points in the network. Finally, relay parameters are optimally tuned based on the predicted fault probability to guarantee seamless coordination among relay operations under various network scenarios. However, the proposed method may not perform effectively in protecting microgrids against high-impedance faults In[27], the authors proposed an optimized approach for current protection of power grids that utilizes local current information. This method dynamically updates the relay operating characteristics based on the grid's operational conditions and distributed generation (DG) outages. This dynamic adaptation enhances the protection's flexibility and optimizes system performance against faults. Building upon this work, the authors in [28 and 29] introduced novel current-time-voltage (I-T-V) tripping characteristics to further improve current protection efficiency. These new characteristics enable faster and more reliable protection by optimizing the total relay operation time. The formulation of these characteristics was framed as a constrained nonlinear programming (NLP) problem based on standard overcurrent protection (OCR) characteristics. Despite the notable advantages of the methods presented in [27, 28, and 29], their effectiveness may be compromised in certain scenarios due to the neglect of diverse grid operational conditions, including fault type, fault magnitude, and pickup current values. For instance, the extensive integration of DGs into

the grid can significantly impact system behavior under fault conditions, which is not fully considered in these approaches. Therefore, it is crucial to continue research in current protection of power grids with a focus on DG integration and considering the diversity of grid operational conditions. The development of adaptive and dynamic protection schemes that can effectively accommodate varying system conditions is of paramount importance. In the research presented in [30 and 31], a novel approach to coordinating directional overcurrent protection relays for the protection of distribution system microgrids in grid-connected and islanded operating modes was introduced. This innovative method effectively addresses the inherent challenges of microgrid protection by employing a fault current limiter at the point of common coupling (PCC). Furthermore, in [32], microgrid protection using directional overcurrent relays and an agent-based communication system was investigated. This approach provides fast and accurate protection against a wide range of faults by relying on dynamic information exchange between the relays. Aiming to address the inherent challenges of protection coordination in microgrids, a novel protection coordination scheme utilizing dual-setting directional overcurrent relays was proposed in [33]. This innovative scheme significantly reduces the complexity and cost of the protection system by eliminating the requirement for fault current limiters. In [34], a novel scheme is proposed to enhance the protection level of meshed microgrids. The scheme is based on the employment of a set of directional overcurrent relays with two settings. In [35], a novel hybrid optimization method based on the integration of the firefly algorithm and linear programming is proposed to enhance the performance of directional overcurrent relays. By leveraging the strengths of both algorithms, this innovative approach can achieve more desirable and time-efficient results compared to traditional methods. In [36], a novel differential protection scheme for microgrid lines was proposed based on the definition of the islanding correlation index in the presence of inverter-based resources. This scheme, utilizing the correlation index, can detect fault conditions in microgrid lines with higher accuracy and speed than traditional protection schemes. In [37], a novel differential protection scheme based on the calculation of line impedances was proposed for active distribution system lines containing inverter-based distributed generation resources. A fault direction-finding algorithm that utilizes the calculation of incremental changes in voltage and current flowing through the lines, along with an adaptive differential protection algorithm for fault detection and protection of microgrid lines and zones, was proposed in [10]. In [38], the authors proposed a novel differential protection scheme for distribution lines based on the calculation of current signal energy. The use of dual settings for the coordination of directional overcurrent relays, employing genetic algorithms to optimize relay settings, was proposed in [39]. However, achieving coordination for a large number of overcurrent relays with dual settings is often challenging. Fault direction identification using a power-based index for microgrid line protection has been investigated in [40]. The proposed scheme identifies faults based on the degree of network unbalance caused by the fault and determines the fault direction based on the direction of negative sequence reactive power flow. Accordingly, the proposed method is capable of satisfactory performance only for asymmetric faults. The use of derivatives of active power flowing through lines for fault direction detection has been investigated in [41]. Although the proposed scheme demonstrates desirable performance in the occurrence of high-impedance faults, its nature may lead to activation during load switching in the network. In [42], the Stockwell transform and deep neural networks were employed for fault detection and localization. The proposed method effectively visualizes the time-frequency information of current and voltage signals, thereby enhancing the speed of fault detection. Nevertheless, the utilization of variable-length windows to generate time-frequency representations for the input signal could potentially reduce redundancy in the time-frequency domain. Furthermore, the computational complexity associated with this approach constitutes another limitation. In [43], an autoregressive technique was proposed for fault detection. High computational speed is one of the advantages of the suggested method. However, this model heavily relies on historical data for accurate predictions, making it susceptible to performance degradation in the presence of data anomalies. Moreover, the computational complexity of the proposed method increases with the number of parameters and data points, which may potentially compromise its accuracy. In [44], fault detection is proposed using zero-sequence current component decomposition to extract fault features. Additionally, a whale optimization algorithm is employed to enhance the decomposition process. Subsequently, shape-based time series analysis utilizing dynamic time warping derivatives is applied for comparison. However, computational complexity poses a limitation to this approach. Fault detection and classification using positive sequence impedance energy calculation is proposed in [45]. A novel fault detection and classification method is proposed in [46], which simultaneously utilizes both temporal and frequency domain variations of current signals and defines a differential index. The weakness of the proposed method lies in its inability to operate under symmetrical fault conditions within the network Studies have shown that most proposed methods for the protection of active distribution systems are based on optimization problems and coordination among multiple relays. This can inherently lead to increased operational time of protection systems. Moreover, achieving coordination among multiple overcurrent relays is challenging. Given that identifying the

direction of an error can simplify both error detection and localization, novel approaches have been introduced in this regard. One such approach is the method proposed in [10]. A limitation of this approach is its inability to identify the direction of fault current flow under single-phase fault conditions. Furthermore, the proposed scheme has been investigated and evaluated for three-phase faults with an impedance of 0.1 ohms. This paper presents a fault direction recognition scheme based on the derivatives of active power flow and the calculation of its energy polarity for the protection of lines and microgrid areas. The objective is to identify the fault current direction resulting from various fault types and to increase the fault impedance value compared to similar methods. Additionally, to prevent the fault direction scheme from being affected by factors such as load switching and the occurrence of faults outside the protection zone, a sub-differential scheme based on the calculation of the transient energy difference of line current signals is proposed. Table 1 presents the results of the study.

The following are the main contributions of this work that demonstrate its novelty for the microgrid protection:

TABLE 1 PERFORMANCE COMPARISON OF THE PROPOSED METHOD WITH EXISTING METHODS

Ref.	direction detection	Operation in island mode	Inverter based sources	High penetration of resources
[24]	×	×	✓	✓
[25]	×	✓	×	✓
[26]	×	✓	✓	✓
[10]	✓	✓	✓	×
[38]	×	✓	✓	×
Proposed Strategy	✓	✓	✓	✓

The proposed directional algorithm offers a straightforward approach to fault detection in lines and areas of a microgrid. This is because it solely relies on the active power flow through lines and areas for fault detection. By utilizing power derivatives, the transient energy of the active power flow can be easily calculated.

The proposed directional algorithm is capable of protecting microgrid lines and areas by effectively distinguishing between internal and external faults

The proposed method is a two-stage protection scheme that employs a differential protection approach based on the energy difference of current signals flowing through lines and areas. This ensures reliable operation in the event of an internal fault within the protected zone while preventing false tripping in the case of external faults or heavy loading conditions.

The proposed directional method is capable of identifying the direction of fault current under various fault conditions and microgrid configurations.

Moreover, the structure of the paper is organized as follows:

Section II introduces the proposed fault direction recognition method and the sub-differential scheme based on the energy difference of signals. Section III evaluates the performance of the proposed methods. Finally, Section IV presents the conclusions.

II. Methodology

A. Fault current direction identification algorithm

The increasing penetration of inverter-based distributed generation resources in distribution systems leads to a significant reduction in system inertia. In this case, the fault current is much lower than in traditional distribution systems that use machine-based distributed generation resources. The significant reduction in fault current in distribution systems with inverter-based distributed generation resources can pose serious challenges to conventional protection methods. Therefore, the proposed algorithms offer a novel and innovative approach to the protection of active distribution systems, which are described below. The presence of distributed generation resources in local distribution systems results in a bidirectional fault current. Therefore, identifying the direction of the fault current at the time of its occurrence is of utmost importance. However, the commonly used sequence components-based directional algorithms presented in [25] may fail for microgrids with inverter-based DERs. This is because inverter-based DERs produce few or no zero- or negative-sequence components during faults. The proposed direction-finding algorithm uses the magnitudes of the power flowing through the microgrid lines and the transient increasing energy of the real power to identify the direction of the fault current at the time of occurrence. To analyze three-phase networks, we consider the following balanced sinusoidal phase and line voltages:

$$\begin{cases} v_a(t) = \sqrt{2}\,V\cos(\omega t + \varphi_V) \\ v_b(t) = \sqrt{2}\,V\cos(\omega t + \varphi_V - \frac{2\pi}{3}) \\ v_c(t) = \sqrt{2}\,V\cos(\omega t + \varphi_V + \frac{2\pi}{3}) \end{cases} \quad (1)$$

$$\begin{cases} i_a(t) = \sqrt{2}\, I\, cos(\omega t + \varphi_I) \\ i_b(t) = \sqrt{2}\, I\, cos(\omega t + \varphi_I - \frac{2\pi}{3}) \\ i_c(t) = \sqrt{2}\, I\, cos(\omega t + \varphi_I + \frac{2\pi}{3}) \end{cases} \quad (2)$$

The phase angles of the voltage and current, φ_V and φ_I, respectively, are represented with respect to a specified reference. The above voltages and currents are characterized by the presence of a sinusoidal component in their positive-sequence components. This indicates that they are sinusoidal and balanced. The voltage and current phasors can be transformed to the stationary reference frame using (3):

$$\begin{bmatrix} v_\alpha \\ v_\beta \end{bmatrix} = \sqrt{\frac{2}{3}} \begin{bmatrix} 1 & -\frac{1}{2} & -\frac{1}{2} \\ 0 & \frac{\sqrt{3}}{2} & -\frac{\sqrt{3}}{2} \end{bmatrix} \begin{bmatrix} v_a \\ v_b \\ v_c \end{bmatrix} \quad (3)$$

Currents can be transformed to a stationary reference frame by using similar equations. In Equation (4), the voltages and currents that have been converted to a fixed reference frame are given.

$$\begin{cases} v_\alpha = \sqrt{3} V cos(\omega t + \varphi_V) \\ v_\beta = \sqrt{3} V sin(\omega t + \varphi_V) \\ i_\alpha = \sqrt{3} I cos(\omega t + \varphi_I) \\ i_\beta = \sqrt{3} I sin(\omega t + \varphi_I) \end{cases} \quad (4)$$

where v_α, v_β, i_α and i_β are the transformed voltages and currents with respect to the reference axes αβ. The Clarke transform and its inverse preserve instantaneous power in three-phase systems. This property makes the Clarke transform a very useful and efficient tool for analyzing instantaneous power in three-phase systems. The instantaneous three-phase active power is calculated using the instantaneous phase voltages and line currents based on Equation (5).

$$P_{3\varphi}(t) = v_a(t) i_a(t) + v_b(t) i_b(t) + v_c(t) i_c(t) \quad (5)$$

The initial definition of p and q as given in [47] is according to Equation (6).

$$\begin{bmatrix} p \\ q \end{bmatrix} = \begin{bmatrix} v_\alpha & v_\beta \\ -v_\beta & v_\alpha \end{bmatrix} \begin{bmatrix} i_\alpha \\ i_\beta \end{bmatrix} \quad (6)$$

The above equation can be employed as a valuable analytical tool for investigating the real power fluctuations in three-phase systems. The fault location algorithm is based on the integral of active power changes that pass through the lines according to Equations (7) and (8).

$$\Delta p = p^{fault} - p^{pre} \quad (7)$$

$$Energy(t) = \int_0^T \Delta p(t) dt \quad (8)$$

In this equation, the change in active power flowing through the protected area is denoted by Δp. The active power flowing through the protected area at the time of the fault and after the fault are denoted by p^{fault} and p^{pre}, respectively. In this algorithm, the active power value in each cycle is compared with that in the three previous cycles to detect changes in the active power flowing through a protected area. The difference between the two values is used to determine whether a fault has occurred. Fig. 1 illustrates the proposed energy algorithm for the protected area.

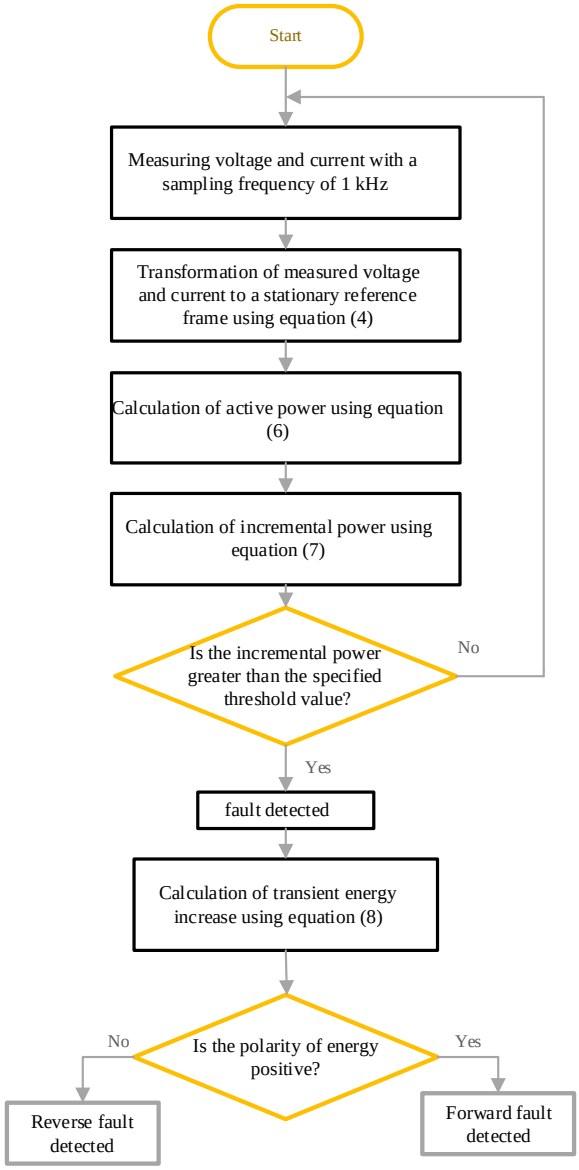

Fig. 1. Fault direction identification algorithm.

The measured voltage and current signals, sampled at a frequency of 1 *kHz*, constitute the input data for the algorithm. If the active power samples exceed the preset threshold for three consecutive samples, a fault is detected. In this paper, the fault detection threshold is set to five

percent of the nominal current. If the polarity of energy is positive, a forward fault is detected. If the polarity of energy is negative, a backward fault is detected. The received energy from both sides of the line is positive in the context of the proposed scheme for a bidirectional transmission line. However, the detection of negative energy polarity on one side of a transmission line indicates an external protection zone fault. In the event of a fault on the middle line of a distribution system, the direction of the fault current from the network to the faulted area is indicated by the positive polarity of upstream energy.

B. Differential protection scheme based on Tiger-Kaiser energy calculation method

Building on Teager's original concept, J. F. Kaiser introduced a straightforward algorithm to compute the energy present in a signal, based on its amplitude and frequency of oscillation. For a continuous sinusoidal signal, as depicted in equation (9), the energy required to generate the signal is proportional to the product of the square of its fundamental frequency and the square of its amplitude.

$$\zeta = \alpha \cos(\omega t + \phi) \tag{9}$$

Where ω and f are the angular frequency and base frequency, respectively.

$$\omega = 2\pi f \tag{10}$$

This energy measure is commonly referred to as the Teager–Kaiser Energy Operator (TKEO) [48]. Furthermore, the derived identity effectively links the Teager–Kaiser energy of the signal with its key parameters, offering a reliable metric for signal energy computation as shown in equation (11).

$$\dot{\zeta}(t)^2 - \zeta(t).\ddot{\zeta}(t) = \alpha^2.\omega^2 \tag{11}$$

The first and second-order derivatives of the signal $\zeta(t)$ are denoted by $\dot{\zeta}(t)$ and $\ddot{\zeta}(t)$, respectively, and play a pivotal role in deriving the mathematical identity associated with signal energy. Therefore, the continuous form of TKEO, is expressed as

$$\psi_{\zeta(t)} = \dot{\zeta}(t)^2 - \zeta(t).\ddot{\zeta}(t) \tag{12}$$

Further, this technique can also be implemented for discrete signal, shown in (13).

$$\zeta[n] = \alpha \cos(\Omega n + \phi) \tag{13}$$

Where Ω represents the digital frequency in radians per sample for the sample n, and ϕ denotes the phase as shown in equation (14).

$$\Omega = \frac{2\pi f}{f_s} \tag{14}$$

In this equation, f_s is the sampling frequency in Hz. The two adjacent points referenced in equation (13) can be represented as a set of equations, as shown in equation (15).

$$\zeta[n-1] = \alpha \cos(\Omega[n-1] + \phi)$$

$$\zeta[n+1] = \alpha \cos(\Omega[n+1] + \phi) \tag{15}$$

To compute the Teager-Kaiser Energy Operator (TKEO) for a discrete-time signal, three consecutive signal samples are required. The resulting energy value is calculated using the expression provided in equation (16).

$$\zeta[n+1].\zeta[n-1] = \zeta[n]^2 - \alpha^2 \sin^2(\Omega) \tag{16}$$

Subject to a small value of ω, the sampling frequency can be increased to more than eight times the signal frequency by imposing a limitation of π/4 on the value of This leads to a reduction in the relative error to 11%. Under these conditions, the energy operator yields a result that is expressed in Equation (17) and represents the energy contained in the signal [40].

$$\zeta[n]^2 - \zeta[n+1].\zeta[n-1] = \alpha^2\Omega^2 \tag{17}$$

Thus, the formulation of the Teager-Kaiser Energy Operator (TKEO) for discrete signals is expressed as presented in equation (18) [38],[48].

$$\psi_{\zeta[n]} = \zeta[n]^2 - \zeta[n+1].\zeta[n-1] \tag{18}$$

It is important to highlight that the TKEO is an efficient algorithm, requiring only two multiplications and one subtraction per data point to estimate the signal energy. This simplicity in computational operations contributes to its speed, making it well-suited for real-time applications and systems where rapid energy estimation is critical.

Fig. 2 presents the schematic diagram of differential current protection operation for a line.

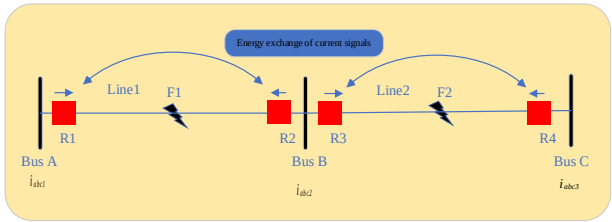

Fig. 2. Performance of the proposed differential scheme for the line under protection.

Under normal operating conditions, the differential current energy between protective relays R1 and R2 at the beginning and end of line j is zero. In the event of a short-circuit fault on line j, the difference between the energy integrals of the current relays at the two ends of the line becomes non-zero, indicating a fault on the protected line. Considering the characteristics of this type of protection, it can be considered an effective method for line protection. However, in situations where the penetration level of distributed generation sources on the system bus is high, the effectiveness of this method will decrease significantly [38].

The implementation of differential protection schemes in an extensive protection zone encompassing sources, loads, lines, and buses necessitates the definition of an operational

threshold for the proposed scheme. This method employs Equations (19) and (20) to calculate the energy of current signals at the inception and termination points of the protected area. Subsequently, Equation (21) is utilized to determine the energy difference between these two signals [38].

$$E_{1(j)p\in a,b,c} = I_{1(j)p}[n]^2 - I_{1(j)p}[n+1] \cdot I_{1(j)p}[n-1] \quad (19)$$

$$E_{2(j+1)p\in a,b,c} = I_{2(j+1)p}[n]^2 - I_{2(j+1)p}[n+1] \cdot I_{2(j+1)p}[n-1] \quad (20)$$

$$Energy_{dif} = E_{1(j)p\in a,b,c} - E_{2(j+1)p\in a,b,c} \quad (21)$$

Exceeding the predetermined threshold of the calculated energy difference confirms the occurrence of a fault within the protected zone. Fig. 3 illustrates the differential current protection algorithm in an extended protection zone. The proposed differential protection scheme, in conjunction with the directional identification algorithm, facilitates the isolation of faulty zones from healthy zones and prevents misoperation of the protective relay. The operating threshold of the differential current protection scheme is determined based on the calculation of fault energy for internal and external faults, considering an allowable load of 10% for the connected state and 5% for the islanded state. This threshold is set to prevent the algorithm from malfunctioning under permissible conditions, such as loading.

I. Test Results

A. Case study system:

To evaluate the performance of the proposed scheme, an active distribution network with a 50 Hz frequency was simulated using the PSCAD software. The data obtained from this simulation was processed and used to implement the proposed algorithms in MATLAB [37]. Fig. 4 illustrates the studied system. The system consists of two 0.4 kV and 10 kV feeders that are connected to the 35 kV main grid via a transformer. The short-circuit capacity at the coupling point of these feeders to the main grid is 500 MVA, and the R/X ratio is 0.1. The nominal powers of the distributed generation (DG) sources in the 0.4 kV feeder are 200 kVA, 100 kVA, and 50 kVA, respectively. The nominal power of the DG source located at the end of the 10 kV feeder is 600 kVA. DG1 is a battery energy storage system (BESS), DG2 is a combined cooling, heating, and power (CCHP) system, and DG3 is a photovoltaic (PV) system connected to the low-voltage feeder. The DG source in the 10 kV feeder is a machine-based source (diesel generator). The positive and negative sequence resistances and inductances of the 0.4 kV feeder are 0.32 Ω/km and 0.261 mH/km, respectively. The zero sequence resistance and inductance of this part of the network are 1.1 Ω/km and 0.955 mH/km, respectively. The nominal powers of loads 1 to 6 in the 0.4 kV (low-voltage) feeder are 40 kVA, 20 kVA, 40 kVA, 40 kVA, 5 kVA, and 25 kVA, respectively. It is worth noting that a shunt capacitor with a nominal reactive power of 20 kVAR is used in one part of the network. The positive and negative sequence resistances and inductances of the 10 kV subnetwork are 0.38 Ω/km and 1.432 mH/km, respectively. The zero sequence resistance and inductance are 0.76 Ω/km and 4.2 mH/km, respectively. The nominal powers of loads 7 to 9 in this part of the network are 100 kVA, 500 kVA, and 500 kVA, respectively. The 0.4 kV feeder consists of inverter-based distributed generation (DG) sources that can supply the loads of this feeder in case of grid islanding during grid restructuring.

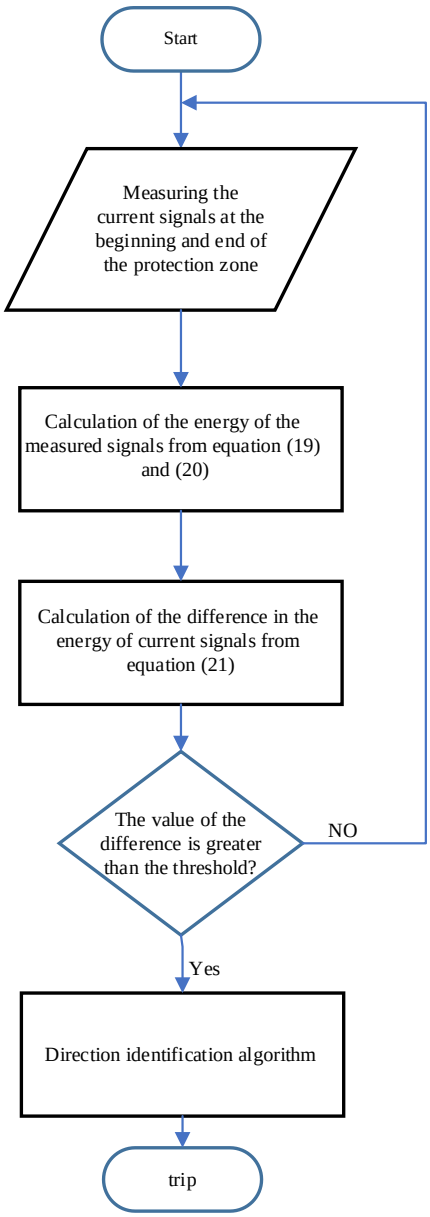

Fig. 3. Energy difference algorithm of current signals.

Table 2 demonstrates a comprehensive comparison between the proposed method and a similar method conducted in [10] for identifying the fault current direction.

The operating mode of energy storage batteries or distributed generation (DG) sources with combined cooling, heating, and power (CCHP) changes from P-Q to V-f control to support voltage and frequency during grid islanding transitions from grid-connected to island mode. However, the operation of photovoltaic (PV) systems is such that P-Q control is maintained in both grid-connected and island modes.

TABLE 2 COMPARISON OF THE PROPOSED DIRECTION IDENTIFICATION METHOD AND THE METHOD PROPOSED IN REFERENCE [10]

		Ref [10]		Proposed Strategy	
Fault resistance	**Fault type**	**Traditional differential**	**Fault direction**	**Energy-based differential**	**Corrected fault direction detection**
0.1 ohm	A-g	✓	×	✓	✓
	BC	✓	✓	✓	✓
	BC-g	✓	✓	✓	✓
	ABC	✓	✓	✓	✓
	ABC-g	✓	✓	✓	✓
20 ohm	A-g	×	×	✓	✓
	BC	×	×	✓	✓
	BC-g	×	×	✓	✓
	ABC	×	×	✓	✓

It is noteworthy that the output current of the inverter-based distributed generation (DG) sources used in this network is limited to 1.5 times the nominal current in case of a fault. It is also worth noting that the data presented in [49] to [51] were used to implement the proposed network.

A. Analysis of Fault Current Behavior

The performance of the proposed scheme for determining fault current direction based on the polarity of the incremental active power, aiming to identify faults inside and outside the protection zone, and the performance of the proposed scheme for the protection of active distribution lines in the following subsections have been investigated.

Case 1: Internal Faults: The performance of the proposed fault current direction detection scheme is depicted in Fig. 5, focusing on a fault event on line 4. Relay 4 acts as the input measurement for the designated protection zone, while Relay 6 serves as the output measurement. Analyzing the directional measurements from these relays reveals that, in scenarios where a fault occurs outside the protection zone or during load switching external to this zone, the energy calculated by both the input and output relays maintains the same polarity. In contrast, when a fault is detected within the protection zone, the input and output relays indicate an incremental energy transient characterized by opposite polarities.

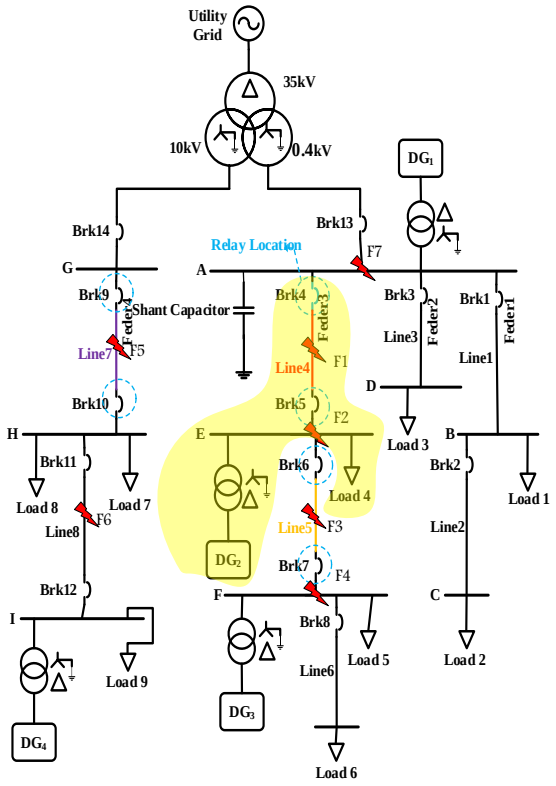

Fig. 4. Case study system.

In Fig. 6, the effectiveness of the proposed approach for identifying the direction of fault current in the event of a fault at bus E is presented. The results shown in Fig. 5 and 6 demonstrate that for faults that occur within the protection zone, the calculated energy polarity at both the beginning and the end of this zone is found to be opposite. This characteristic serves as a significant indicator for recognizing internal faults and can be considered a reliable standard for measuring the effectiveness of the zone protection system. Moreover, the proposed index is capable of identifying faults occurring within the distribution lines of active distribution systems. Considering relays 4 and 5 as the beginning and end relays of line 4, respectively, whenever a fault occurs on line 4, the energy polarity of the relays at the beginning and end of the protected line is positive, indicating a fault ahead of the protective relays. As evident from Fig. 5, for a fault occurring on line 4, the calculated transient energy polarity at both the beginning and end of the line is positive.

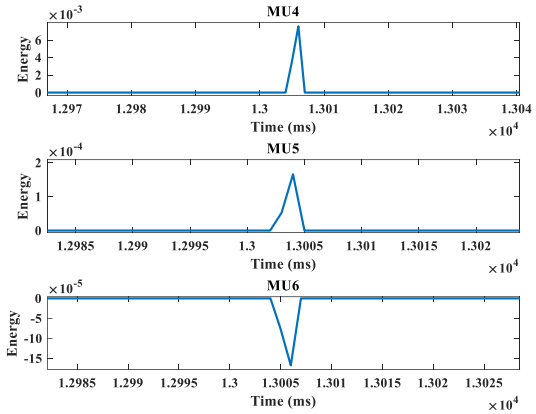

Fig. 5. Performance of the directional protection scheme under three-phase fault conditions on line 4 in grid connected mode.

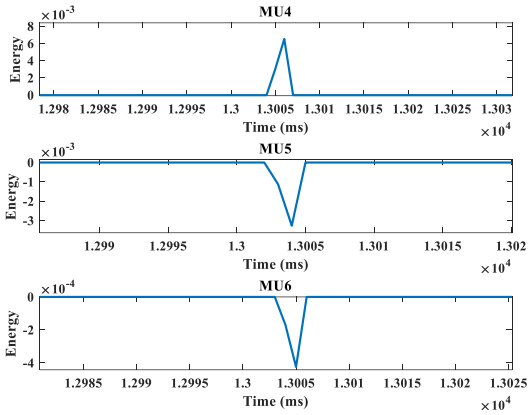

Fig. 6. Performance of Directional Protection Scheme under a Single Line-to-Ground Fault (A-G) on Bus E in Grid-Connected Mode.

However, as clearly shown in Fig. 6, for a fault occurring outside the line, the energy polarity of the incoming relay is positive, indicating a fault current flow direction from the network towards the downstream. Under such conditions, the calculated energy polarity for the outgoing relay is negative, indicating a fault behind the relay. Fig. 7 illustrates the identification of the fault direction on line 4 as an internal fault.

As shown in Fig. 7, when a fault occurs on bus E, the calculated energy polarity by the relay at the beginning of line 4 is positive, and the energy polarity for the relay at the end of the line is negative. This condition indicates a fault outside the line. Additionally, since the fault occurs within the protected zone, the energy polarity of relay 4 is positive and the energy polarity of relay 6 is negative, which indicates a fault within the protected zone. The results demonstrate that the proposed scheme is capable of accurately and rapidly detecting faults within the protected zone.

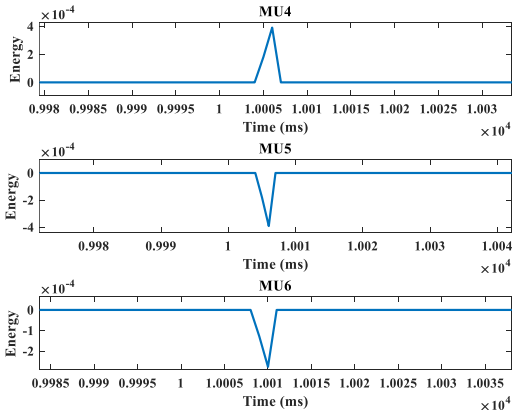

Fig. 7. Performance of Directional Protection Scheme under a Double Line-to-Ground Fault (AB-G) on Bus E in Islanded Mode.

Case 2: External faults: One of the distinguishing features of the proposed method is its ability to differentiate between faults inside and outside the protection zone. Fig. 8 illustrates the performance of the directional protection scheme when a fault occurs outside the protection zone. As evident from Fig. 8, when a fault occurs on line 5, the energy polarity calculated by relay 4 is positive, indicating a fault ahead of the relay. In this situation, the energy polarity calculated by relay 5 is negative, confirming a fault outside line 4. Moreover, the positive energy polarity of the outgoing relay corroborates the occurrence of a fault outside the protection zone. Fig. 9 presents the results of fault current direction finding under fault conditions outside the protection zone during islanding mode operation.

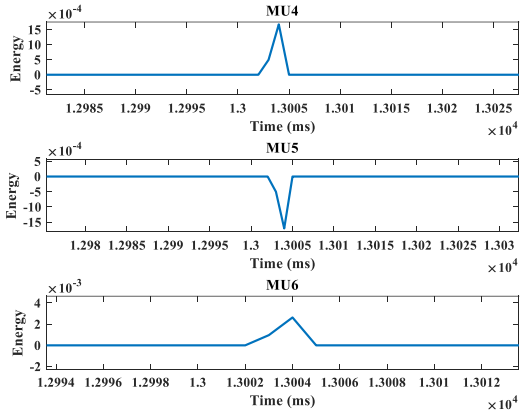

Fig. 8. Performance of the directional protection scheme under a single-phase-to-ground fault (B-G) on line 5 in grid-connected mode.

As evident from Fig. 9, when a fault occurs on bus A, the energy polarity measured by relay 4 is negative. This indicates that the fault current direction is from the load side

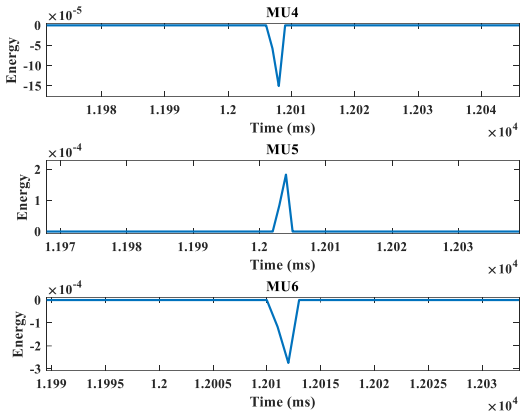

Fig. 9. Performance of the directional protection scheme under a three-phase fault on bus A during islanding mode operation.

towards the source. Under such conditions, the energy polarity of relay 5 is positive, implying a fault outside the protected line. Furthermore, the negative polarity of relay 6 confirms that the fault is located outside the protection zone. Fig. 10 illustrates the operational performance of the proposed directional scheme in response to an external fault occurring on line 8.

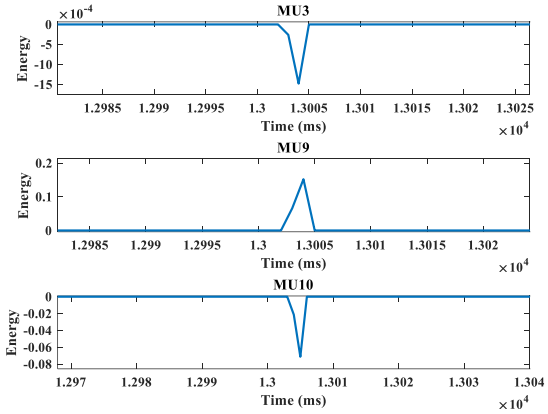

Fig. 10. Performance of the proposed directional scheme under single-phase fault conditions (A-G) in grid-connected mode on line 8.

As illustrated in Fig. 10, it can be observed that in the case of a fault occurring on line 8, relay number 3, which operates with negative polarity, is able to identify the fault occurring behind it. Therefore, should a fault arise at any location within the network, all relays will react in a positive or negative manner depending on the fault's position. This capability is particularly beneficial for accurately locating the fault. Furthermore, on line 7, the first relay exhibiting positive polarity and the last relay exhibiting negative polarity indicate the existence of a fault external to the line. Based on the results obtained from the execution of the directed protection scheme under fault conditions within the microgrid, it is evident that the proposed approach is adequately equipped to detect faults and differentiate between internal and external faults in the designated protection zone. The assessment was conducted with a fault impedance of 20 ohms, and the fault identification time was 5 milliseconds post-occurrence.

B. Current Differential Protection Scheme

In this section, the performance of the proposed differential protection scheme is evaluated for detecting and discriminating faults both inside and outside the protection zone, while considering network loading conditions.

Case 1: Internal Faults: Fig. 11 demonstrates the operation of the proposed design when faults occur within the protected region.

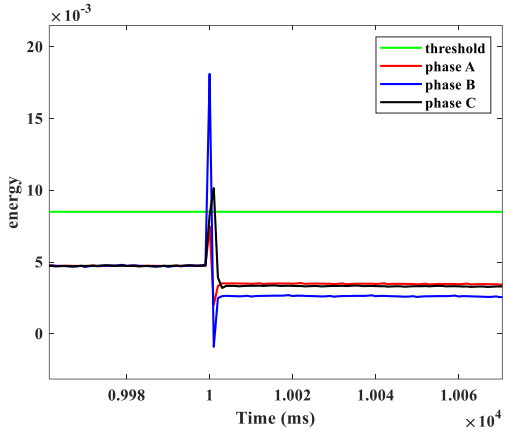

Fig. 11. Performance of the proposed scheme under three-phase fault conditions on Line 4 in grid-connected mode.

While noise in transmitted data is commonly considered in transmission lines, its impact is often overlooked in distribution networks where line lengths are shorter. Specifically, when a differential scheme is employed for short lines, susceptibility to noise can become a significant drawback of the proposed design. Fig. 12 illustrates the performance of the proposed scheme under fault conditions in islanded mode. When a fault occurs at 10 seconds, the difference in energy of the current signals exceeds the threshold, which can serve as a suitable criterion for determining a fault within the protection zone. The results clearly indicate that, following a fault within the protected zone, the difference in energy of the current signals entering and exiting the protected zone can serve as a reliable criterion for fault detection.

Case 2: External faults and load switching: One of the advantages of the proposed method is its immunity to external faults and load switching operations outside the protection zone. Fig. 13 illustrates the performance of the proposed scheme under fault conditions, both inside and

outside the protection zone. Fig. 14. depicts the performance of the proposed scheme under fault conditions on busbar F in islanded mode. The results clearly demonstrate the proposed scheme's ability to discriminate between faults inside and outside the protection zone.

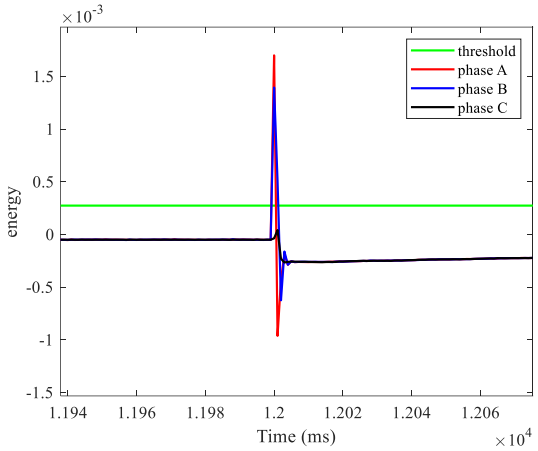

Fig. 12. Performance of the proposed scheme under an AB-G phase-to-ground fault condition on Line 4 in island mode.

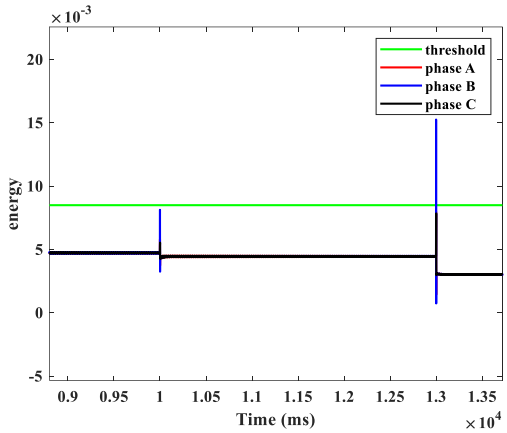

Fig. 13. Performance of the proposed scheme under a three-phase fault with an impedance of 0.1 ohms on line 5 at the 10th second, and a three-phase fault with an impedance of 20 ohms on line 4 at the 13th second in grid-connected mode.

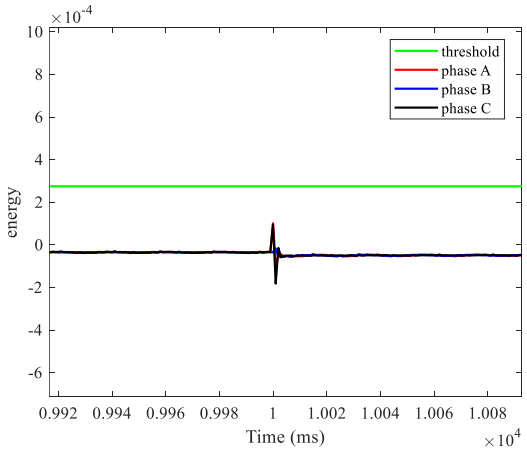

Fig. 14. Performance of the proposed scheme under three-phase fault condition on busbar F in islanded mode.

Fig. 15. illustrates the performance of the differential protection scheme under a single-phase fault outside the protection zone.

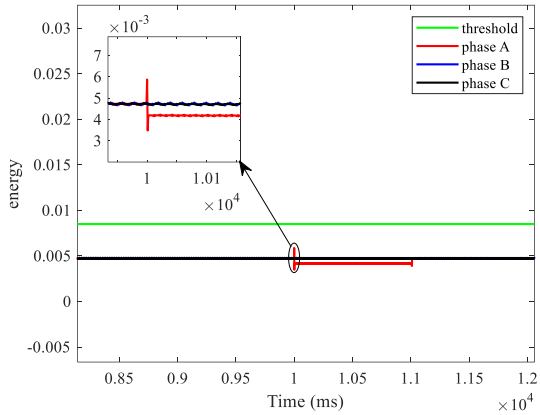

Fig. 15. The performance of the proposed scheme under single-phase (A-G) fault conditions on Line 5 in grid-connected mode.

As seen in the figure, when a fault occurs at the 10th second, the energy difference between the current signals becomes greater than under normal conditions. However, this difference is not sufficient to cause the proposed scheme to operate. The performance of the proposed scheme has been evaluated for internal faults within the protection zone with a fault impedance of 20 ohm and for external faults outside the protection zone with an impedance of 0.1 ohm.

Given that the algorithm employed to calculate the energy of current signals passing through the protection zones exhibits high accuracy and speed in tracking sinusoidal signals, the transit time resulting from the difference between the signal energy and the defined threshold is extremely short. Since this scheme is a sub-algorithm to complement the directional algorithm, it is reliable. The fault detection time for this algorithm is 3 milliseconds. Therefore, in addition to ease of calculation, the high speed and accuracy of the method used are confirmed by the obtained results.

Given that the proposed directional fault current algorithm is highly sensitive to variations in active power flow, it is imperative that the suggested sub-algorithm remains unaffected by such changes. As evident from Fig. 16, load switching results in a difference in the energy of current signals that deviates from the normal state. However, by defining a threshold and allowable load levels (10% of the load level both outside and inside the protected zone), the proposed scheme can effectively differentiate between loading conditions.

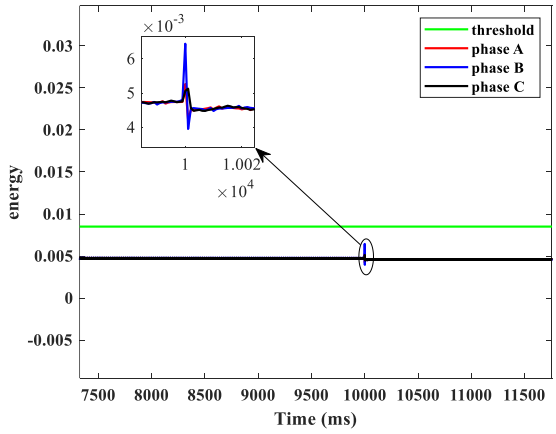

Fig. 16. Performance of the proposed scheme under increased load at bus F in grid-connected mode.

Fig. 17 illustrates the proposed scheme's ability to differentiate between load switching and fault occurrences within the protected zone during islanded operation. The results indicate that the proposed scheme, by determining an appropriate threshold in both grid-connected and islanded operation modes, can distinguish between faults within the protection zone and loads outside the protection zone.

While directional protection schemes offer superior speed, accuracy, and reliability for safeguarding areas containing distributed generation and loads, results have shown that the energy differential of current signals is effective only for internal faults. Given the proposed directional protection scheme's high sensitivity to active power variations, the energy-based differential algorithm can be employed as a supplementary method for external faults and load-switching conditions within the network.

A similar adaptive differential protection and direction-finding algorithm was employed in [10], but it exhibited limitations in identifying the fault current direction under single-phase fault conditions and had a detection capability for faults with an impedance of 0.1 ohms. Based on the obtained results, the proposed schemes have proven suitable for identifying various fault types under different microgrid operating conditions and have improved the impedance detection capability to 20 ohms compared to the similar method.

III. Conclusions

This paper presents a novel fault direction-finding scheme for the protection of lines and zones, leveraging incremental changes in active power flow. To prevent false operations during external faults and load switching events, a complementary differential protection scheme based on the energy of current signals is utilized. The Teager-Kaiser Energy Operator (TKEO) is employed to extract the energy from current signals at both ends of the line, and fault detection is accomplished by evaluating the energy difference between these signals. The results confirm that the proposed directional scheme accurately determines fault current direction under a variety of fault conditions, enabling rapid and precise discrimination between internal and external faults within the protected zone or line in diverse microgrid configurations. Additionally, the proposed methods demonstrate superior performance in handling higher fault impedances compared to existing directional schemes. Future work should investigate the impact of harmonics within microgrids on the proposed methodology.

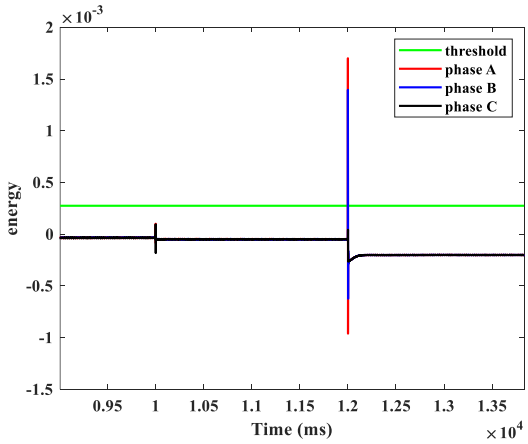

Fig. 17. Performance of the proposed scheme during a load increase at bus F at seconds10 and a three-phase fault at bus E at seconds12 under islanded operation.

References

[1] X. Kang, C. E. Nuworklo, B. S. Tekpeti, and M. Kheshti, "Protection of micro - grid systems: a comprehensive survey," The Journal of Engineering, vol. 2017, no. 13, pp. 1515-1518, 2017.

[2] S. Alzahrani, K. Sinjari, and J. Mitra, "An advanced control and protection integration scheme for microgrids," Sustainable Energy, Grids and Networks, vol. 32, p. 100940, 2022

[3] H. J. Laaksonen, "Protection principles for future microgrids," IEEE Transactions on power electronics, vol. 25, no. 12, pp. 2910-2918, 2010.

[4] M. R. Miveh, M. Gandomkar, S. Mirsaeidi, and M. R. Gharibdoost, "A review on protection challenges in microgrids," in 2012 Proceedings of 17th Conference on Electrical Power Distribution, 2012: IEEE, pp. 1-5.

[5] H. Nikkhajoei and R. H. Lasseter, "Microgrid protection," in 2007 IEEE Power Engineering Society General Meeting, 2007: IEEE, pp. 1-6.

[6] H. Hooshyar, M. Baran, S. R. Firouzi, and L. Vanfretti, "PMU-assisted overcurrent protection for distribution feeders employing Solid State Transformers," Sustainable Energy, Grids and Networks, vol. 10, pp. 26-34, 2017

[7] A. Salam, A. Mohamed, and M. Hannan, "Technical challenges on microgrids," ARPN Journal of engineering and applied sciences, vol. 3, no. 6, pp. 64-69, 2008.

[8] E. Sortomme, S. Venkata, and J. Mitra, "Microgrid protection using communication-assisted digital relays," IEEE Transactions on Power Delivery, vol. 25, no. 4, pp. 2789-2796, 2009.

[9] A. Hooshyar and R. Iravani, "Microgrid protection," Proceedings of the IEEE, vol. 105, no. 7, pp. 1332-1353, 2017.

[10] A. C. Adewole, A. D. Rajapakse, D. Ouellette, and P. Forsyth, "Protection of active distribution networks incorporating microgrids with multi-technology distributed energy resources," Electric Power Systems Research, vol. 202, p. 107575, 2022.

[11] A. Narimani and H. Hashemi-Dezaki, "Optimal stability-oriented protection coordination of smart grid's directional overcurrent relays based on optimized tripping characteristics in double-inverse model using high-set relay," International Journal of Electrical Power & Energy Systems, vol. 133, p. 107249, 2021.

[12] A. Reda, A. F. Abdelgawad, and M. Ibrahim, "Effect of non standard characteristics of overcurrent relay on protection coordination and maximizing overcurrent protection level in distribution network," Alexandria Engineering Journal, vol. 61, no. 9, pp. 6851-6867, 2022.

[13] P. Thararak and P. Jirapong, "Implementation of optimal protection coordination for microgrids with distributed generations using quaternary protection scheme," Journal of Electrical and Computer Engineering, vol. 2020, pp. 1-13, 2020.

[14] A. Dagar, P. Gupta, and V. Niranjan, "Microgrid protection: A comprehensive review," Renewable and Sustainable Energy Reviews, vol. 149, p. 111401, 2021.

[15] A. Hatata, A. Ebeid, and M. El-Saadawi, "Application of resistive super conductor fault current limiter for protection of grid-connected DGs," Alexandria engineering journal, vol. 57, no. 4, pp. 4229-4241, 2018.

[16] D. S. Kumar and D. Srinivasan, "A numerical protection strategy for medium-voltage distribution systems," in 2018 IEEE Innovative Smart Grid Technologies-Asia (ISGT Asia), 2018: IEEE, pp. 1056-1061.

[17] F. B. dos Reis, J. O. C. Pinto, F. S. dos Reis, D. Issicaba, and J. G. Rolim, "Multi-agent dual strategy based adaptive protection for microgrids," Sustainable Energy, Grids and Networks, vol. 27, p. 100501, 2021.

[18] E. C. Piesciorovsky and N. N. Schulz, "Comparison of Programmable Logic and Setting Group Methods for adaptive overcurrent protection in microgrids," Electric Power Systems Research, vol. 151, pp. 273-282, 2017.

[19] S. D. Saldarriaga-Zuluaga, J. M. Lopez-Lezama, and N. Munoz-Galeano, "Optimal coordination of over-current relays in microgrids considering multiple characteristic curves," Alexandria Engineering Journal, vol. 60, no. 2, pp. 2093-2113, 2021.

[20] R. Sitharthan, M. Geethanjali, and T. K. S. Pandy, "Adaptive protection scheme for smart microgrid with electronically coupled distributed generations," Alexandria Engineering Journal, vol. 55, no. 3, pp. 2539-2550, 2016.

[21] Q. Jia, X. Dong, and S. Mirsaeidi, "A traveling-wave-based line protection strategy against single-line-to-ground faults in active distribution networks," International Journal of Electrical Power & Energy Systems, vol. 107, pp. 403-411, 2019.

[22] M. Išlić, S. Sučić, J. Havelka, and A. Marušić, "Centralized radial feeder protection in electric power distribution using artificial neural networks," Sustainable energy, grids and networks, vol. 22, p. 100331, 2020.

[23] D. Orazgaliyev, A. Tleubayev, B. Zholdaskhan, H. K. Nunna, A. Dadlani, and S. Doolla, "Adaptive coordination mechanism of overcurrent relays using evolutionary optimization algorithms for distribution systems with DGs," in 2019 International Conference on Smart Energy Systems and Technologies (SEST), 2019: IEEE, pp. 1-6.

[24] S. D. Saldarriaga-Zuluaga, J. M. López-Lezama, and N. Muñoz-Galeano, "Adaptive protection coordination scheme in microgrids using directional over-current relays with non-standard characteristics," Heliyon, vol. 7, no. 4, 2021.

[25] H. Liang, H. Li, and G. Wang, "A Single-Phase-to-Ground Fault Detection Method Based on the Ratio Fluctuation Coefficient of the Zero-Sequence Current and Voltage Differential in a Distribution Network," IEEE Access, vol. 11, pp. 7297-7308, 2023.

[26] A. Ataee-Kachoee, H. Hashemi-Dezaki, and A. Ketabi, "Optimized adaptive protection coordination of microgrids by dual-setting directional overcurrent relays considering different topologies based on limited independent relays' setting groups," Electric Power Systems Research, vol. 214, p. 108879, 2023.

[27] P. Mahat, Z. Chen, B. Bak-Jensen, and C. L. Bak, "A simple adaptive overcurrent protection of distribution systems with distributed generation," IEEE Transactions on Smart Grid, vol. 2, no. 3, pp. 428-437, 2011.

[28] A. Hussain and H.-M. Kim, "A hybrid framework for adaptive protection of microgrids based on IEC 61850," International Journal of Smart Home, vol. 10, no. 5, pp. 285-296, 2016.

[29] H. Laaksonen, D. Ishchenko, and A. Oudalov, "Adaptive protection and microgrid control design for Hailuoto Island," IEEE Transactions on Smart Grid, vol. 5, no. 3, pp. 1486-1493, 2014.

[30] E. Dehghanpour, H. K. Karegar, R. Kheirollahi, and T. Soleymani, "Optimal coordination of directional overcurrent relays in microgrids by using cuckoo-linear

optimization algorithm and fault current limiter," IEEE Transactions on Smart Grid, vol. 9, no. 2, pp. 1365-1375, 2016.

[31] W. K. Najy, H. H. Zeineldin, and W. L. Woon, "Optimal protection coordination for microgrids with grid-connected and islanded capability," IEEE Transactions on industrial electronics, vol. 60, no. 4, pp. 1668-1677, 2012.

[32] M. H. Cintuglu, T. Ma, and O. A. Mohammed, "Protection of autonomous microgrids using agent-based distributed communication," IEEE Transactions on Power Delivery, vol. 32, no. 1, pp. 351-360, 2016.

[33] H. M. Sharaf, H. H. Zeineldin, and E. El-Saadany, "Protection coordination for microgrids with grid-connected and islanded capabilities using communication assisted dual setting directional overcurrent relays," IEEE Transactions on Smart Grid, vol. 9, no. 1, pp. 143-151, 2016.

[34] M. N. Alam, R. Gokaraju, and S. Chakrabarti, "Protection coordination for networked microgrids using single and dual setting overcurrent relays," IET Generation, Transmission & Distribution, vol. 14, no. 14, pp. 2818-2828, 2020.

[35] S. P. Ramli, H. Mokhlis, W. R. Wong, M. A. Muhammad, and N. N. Mansor, "Optimal coordination of directional overcurrent relay based on combination of Firefly Algorithm and Linear Programming," Ain Shams Engineering Journal, vol. 13, no. 6, p. 101777, 2022.

[36] A. Saber, H. Zeineldin, T. H. EL-Fouly, and A. Al-Durra, "A signed correlation index-based differential protection scheme for inverter-based islanded microgrids," International Journal of Electrical Power & Energy Systems, vol. 145, p. 108721, 2023.

[37] S. M. Nobakhti, A. Ketabi, and M. Shafie-khah, "A new impedance-based main and backup protection scheme for active distribution lines in ac microgrids," Energies, vol. 14, no. 2, p. 274, 2021.

[38] A. Chandra, G. Singh, and V. Pant, "A novel protection strategy for microgrid based on estimated differential energy of fault currents," Electric Power Systems Research, vol. 214, p. 108824, 2023.

[39] A. H. Ataee-Kachoee, H. Hashemi Dezaki, and A. Ketabi, "Optimized Microgrid Protection Considering Different Topologies Based on N-1 Contingency by Dual Setting Directional Overcurrent Relays," International Journal of Industrial Electronics Control and Optimization, vol. 5, no. 3, pp. 205-213, 2022.

[40] F. Özveren and Ö. Usta, "A power based integrated protection scheme for active distribution networks against asymmetrical faults," Electric Power Systems Research, vol. 218, p. 109223, 2023.

[41] Q. Lai, Z. Zhang, K. Xu, and X. Yin, "A new method of fault direction identification for different types of renewable energy source integrations," IEEE Transactions on Power Delivery, vol. 37, no. 4, pp. 2932-2941, 2021.

[42] L. KANDASAMY and K. Jaganathan, "Intelligent protection scheme using combined Stockwell-Transform and deep learning-based fault diagnosis for the active distribution system," Turkish Journal of Electrical Engineering and Computer Sciences, vol. 32, no. 2, pp. 234-250, 2024.

[43] A. R. Adly and M. E. Rezk, "Optimal Protection Scheme for Distribution Systems Integrated with Distributed Generator," Arab Journal of Nuclear Sciences and Applications, vol. 57, no. 1, pp. 100-106, 2024.

[44] L. Wang, X. Song, and W. Jiang, "Differential protection scheme for distribution network with distributed generation based on improved feature mode decomposition and derivative dynamic time warping," Frontiers in Energy Research, vol. 12, p. 1369880, 2024.

[45] K. Dubey and P. Jena, "Novel Fault detection & classification index for active distribution network using differential components," IEEE Transactions on Industry Applications, 2024.

[46] Z. Moravej, A. Ebrahimi, and M. Barati, "A new differential protection scheme based on Synchro-squeezing transform applied to AC Micro-Grid," Electric Power Systems Research, vol. 231, p. 110336, 2024.

[47] L. S. Czarnecki, "Comparison of power definitions for circuits with nonsinusoidal waveforms," IEEE Tutorial Course 90EH0327-7-PWR, pp. 43-50, 1990.

[48] J. F. Kaiser, "On a simple algorithm to calculate the'energy'of a signal," in International conference on acoustics, speech, and signal processing, 1990: IEEE, pp. 381-384.

[49] W. Huang, T. Nengling, X. Zheng, C. Fan, X. Yang, and B. J. Kirby, "An impedance protection scheme for feeders of active distribution networks," IEEE transactions on power delivery, vol. 29, no. 4, pp. 1591-1602, 2014.

[50] H. J. Laaksonen, "Protection principles for future microgrids," IEEE Transactions on power electronics, vol. 25, no. 12, pp. 2910-2918, 2010.

[51] G. Benmouyal et al., "IEEE standard inverse-time characteristic equations for overcurrent relays," IEEE Transactions on Power Delivery, vol. 14, no. 3, pp. 868-872, 1999.

Reza Karimi was born in Esfahan**,** Iran**.** He received his B.S.c degree in Electrical Engineering from Shahid Rajaee Kashan National University of Skill and his M.S.c degree in Power Electrical Engineering from University of Kashan in 2021 and 2024, respectively. He has been a lecturer at National University of Skill since 2022. His research interests include microgrid protection and power electronics.

Abbas Ketabi received his B.Sc. and M.Sc. degrees in electrical engineering from the Department of Electrical Engineering, Sharif University of Technology, Tehran, Iran, in 1994 and 1996, respectively. He received his Ph.D. degree in electrical engineering jointly from Sharif University of Technology and the Institute National Polytechnique de Grenoble (INPG), Grenoble, France, in 2001. Since 2001, he has been at the University of Kashan, Department of Electrical Engineering. He is currently a Full Professor. He has published more than 130 technical papers and 6 books. He is the Director-in-Charge and editor of the "Energy Engineering and Management" journal. Dr. Ketabi was the recipient the University of Kashan Award for Distinguished Teaching and research. His research interests include power system restoration, power system protection, smart grids, renewable energy, optimization of electric machines, power electronics, and evolutionary computation.

Seyyed Mohammad Nobakti was born in Kashan, Iran, in 1985. He received his M.S. degree from the Faculty of Engineering at Shahed University, Tehran, Iran, in 2011. He obtained his Ph.D. in Electrical Engineering from the Department of Electrical and Computer Engineering at the University of Kashan, Kashan, Iran, in 2021. He is an instructor in the Department of Electrical Engineering at the National University of Skills (NUS) in Tehran, Iran. His current research interests include power electronics and protection in power systems.